

Optimization of Scientific Equipment Pointing at Survey Targets in the Uragan Experiment On Board the ISS¹

M. Yu. Belyaev^{a, b, *}, P. A. Borovikhin^a, A. M. Esakov^a, D. Yu. Karavaev^a, and I. V. Rasskazov^a

^a S.P. Korolev Rocket and Space Corporation “Energia”, PJSC, Korolev, Moscow Region, Russia

^b Bauman Moscow State Technical University, Mytishchi, Moscow Region, Russia

*e-mail: mikhail.belyaev@rsce.ru

Received September 28, 2023; revised October 20, 2023; accepted December 20, 2023

Abstract—The aim of the Uragan space experiment on board the International Space Station (ISS) is to adjust the scientific equipment and improve the methods for monitoring various objects and phenomena on the Earth. Part of this scientific equipment is already operated on board the station, and the other part is planned to be delivered in the orbit soon. In contrast to the Russian orbital stations Salyut and Mir, the ISS was not designed for pointing the installed equipment at the survey targets, because the gyrodines used on the American segment for the ISS attitude control had a too small kinematic momentum. For this reason, special methods and devices had to be developed for pointing the Uragan scientific equipment at the survey targets. This paper considers the methods for pointing the scientific equipment, which would optimize the research program of the Uragan experiment on board the ISS.

Keywords: International Space Station (ISS), Uragan space experiment, scientific equipment, pointing, optimization, steerable platform

DOI: 10.1134/S207510872470007X

INTRODUCTION

At present, space experiments in various research areas are being run on board the ISS. On the orbital stations Salyut and Mir, the experiments within the Russian research program were traditionally conducted in all research areas [1]. In a large number of these experiments, it was necessary to point the scientific equipment at the survey targets. The ISS mission takes place in quasi-orbital attitude, and it is almost impossible to rotate the station for the experimental purposes. This is explained by the fact that the gyrodines of the American segment have a small value of available kinematic momentum. The reasons for this ISS mission mode are as follows. For the NASA and other participants of the project implemented by the ISS American segment, the main scientific task was to investigate microgravity and to conduct medical experiments at the station. These experiments do not require any special attitude of the ISS; it should be orientated in the orbital coordinate frame so that the gravitational perturbing moment is close to zero. The ISS attitude is controlled by means of gyrodines installed on the American segment of the ISS, and by means of thrusters on the Russian segment (RS) of the station. It should be noted that the use of gyrodines for

controlling the attitude of large spacecraft is associated with serious problems, mainly due to the large moments of inertia of these spacecraft, including the ISS. The available kinematic momentum of four gyrodines of the ISS American segment is 19 000 N·m·s, which can only maintain the station attitude in the orbital coordinate frame when the main axes of the ISS inertia are matched with the axes of the orbital frame. For the ISS rotation or arbitrary attitude setting, the orientation, thrusters of the ISS RS can be generally used as actuators, but this will be too fuel-consuming. Therefore, it is virtually impossible to point the devices fixed tightly to the ISS by rotating the station.

The ISS flight mode in use required special methods to be designed for pointing the scientific equipment of the RS at the survey targets. In the case of the Uragan space experiment aimed at studying the targets on the Earth, different approaches were developed for pointing the scientific equipment. Some of the Uragan devices, such as photographic (PSS) and video spectral systems (VSS), as well as photo equipment with large focal distance have a narrow field of view [2]. Initially these devices could be pointed at the survey targets only by the station crew members, so the scope of investigations was limited. In order to point this equipment at the survey targets automatically, it is necessary to use steerable pointing platforms (SPP) [3]. The

¹The article is based on the plenary paper presented at the XXX St. Petersburg International Conference on Integrated Navigation Systems, 2023.

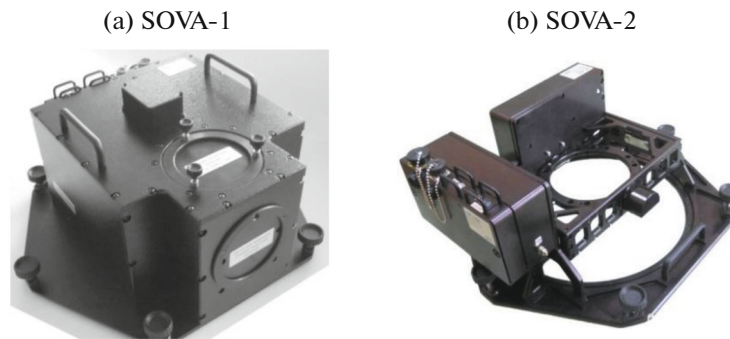


Fig. 1. Steerable pointing platforms.

devices with a relatively large field of view (e.g., the RIVR high-resolution infrared radiometer designed within the Uragan program, or photo equipment with a large field of vision) are pointed due to the ISS motion along the orbit and the station orbit precession. In this case, the scientific equipment is fixed rigidly to the station hull [2].

In the Uragan program, some of the devices rigidly fixed to the station hull, such as ICARUS equipment and RIVR radiometer, can operate in automatic mode. The team of the ISS RS installs the Hyperspectrometer scientific equipment on the porthole no. 9 to perform the surveys. It is not necessary to rotate the ISS in order to point the RIVR and Hyperspectrometer equipment at the survey targets; however, these devices consume the resources of the station: the crew's time for preparatory and final operations with the scientific equipment to perform the experiment; the memory capacity of the recording units, etc., and this should be kept in mind when planning the observations using these devices [2, 4].

Since there are a lot of targets to observe, a possibility for different combinations of the observation priorities, a possibility for simultaneous use of a few sets of SPP on different portholes, a large volume of existing and developing scientific equipment of the Uragan program (VSS, PSS, photo equipment, the Hyperspectrometer, the RIVR infrared radiometer etc.), as well as limitations on the observation capabilities and required resources, it becomes necessary to optimize the observations planning.

To solve these tasks, precise methods and algorithms have been developed, which provide approximated solutions in the cases when precise solutions require unacceptable computational costs. Full or partial similarities with the vehicle routing problems are used, in particular, with multiple travelling salesmen problem (mTSP) [5]. The precise method is usually based on the selection of optimal combinations of observation programs, using the methods of integer linear programming, from the sets of all possible programs that are formed in advance for each device, taking into account the specified limitations. The approx-

imated methods are based on the genetic and ant colony optimization (ACO) metaheuristics.

The presented methods are implemented in special software of the ISS experiments and are used for optimal planning and execution of photo and spectrometric surveys of the Earth surface. The scientific equipment can be simultaneously pointed in the automatic mode by means of SPP installed on the portholes inside the inhabited room of the station.

USE OF SPP FOR POINTING THE SCIENTIFIC EQUIPMENT AT THE TARGETS STUDIED FROM THE ISS RS

At the initial stage of the ISS mission, the scientific equipment was pointed at the survey targets by the station crew [2, 6]. There are certain advantages in the astronauts' involvement in the investigation process. Unfortunately, the astronauts are not able to be on such a "scientific duty" all the time, because they have to do other work most of the day and have a rest at night.

In order to expand the capabilities for target programs implementation on board the station, RSC Energia in cooperation with the Sevchenko Institute of Applied Physical Problems (Belarus) have designed special SPP (Fig. 1) within the Uragan program for the Earth research experiment implemented on board the ISS RS. These SPP SOVA are used for installing different scientific equipment on the portholes of the ISS RS service module and the ISS multirole laboratory module (MLM), and for conducting the surveys according to a specified procedure with or without the operator's participation.

The SOVA system comprises an SPP installed on a porthole; survey equipment and a control laptop located at a distance of 1.5–3 m from the porthole are mounted on this platform. The SOVA system makes it possible to point the fields of view of the scientific equipment and to monitor the object by its image on the laptop display.

There are several versions of the SOVA equipment to be installed in the ISS RS.



Fig. 2. Powell dam, USA.

The SOVA-228 SPP is mounted on the porthole with a diameter of 228 mm in the ISS RS service module and can rotate the installed scientific equipment at ± 180 deg about the axis of sight and point it with at least 20 deg angle of deviation from the optical axis of the porthole in one plane.

The SOVA-426 SPP is mounted on the porthole with a diameter of 426 mm both in the ISS RS service module and multi-purpose lab module, and can point the survey equipment along two orthogonal axes with the deviation angles of at least ± 30 deg.

At the design stage, two structural options for SOVA SPP were considered. The SOVA-1 SPP option (Fig. 1a) is designed as follows. The survey equipment is fixed fast to the SPP, and the Earth surface is scanned by means of a mirror on a suspension which is rotated by electric drives.

The SOVA-2 SPP option (Fig. 2b) has a classical design based on the previous pointing systems. Linear actuators are used as the electric drives rotating the installed equipment.

The angular velocity of the optical axes of the SOVA-1 and SOVA-2 SPP is 0.75–1.5 deg/s and 0.5–6.0 deg/s, respectively.

Although the pointing capabilities of such “internal” platforms in the ISS RS are generally limited compared to the potential capabilities of external SPP, it should be noted that they also have some important advantages, first of all, inexpensiveness and easy maintenance. One of these SPP already works on board the ISS RS, and two more SOVA platforms were delivered to the station this year and are being prepared for use. The SOVA SPP ensure that the VSS instruments and photo equipment are pointed at the survey targets in the automatic mode. Characteristics and capabilities of the VSS scientific equipment are described in [7–9]. Digital cameras Nikon D3X and

Nikon 800 used in the Uragan program produce colored photos with a resolution up to 2 m. Examples of photos taken from onboard the ISS RS are shown in Figs. 2–5.

The SPP application expands significantly the ISS capabilities for researching the Earth and the celestial sphere. In this case, methods of optimal planning of the research experiments program can be used for observing the specified targets. The optimization methods ensure that the maximum volume of useful scientific information will be obtained if certain limitations on planning are fulfilled.

It should be noted that the optimization tasks are set in different fields of science and engineering. For example, the multiple travelling salesmen problem is solved to ensure optimal automated centralized planning of search for fish clusters using several unmanned boats, and in this context, both an accurate method (based on the idea of dynamic programming of the Held-Karp algorithm modification) and a more rapid approximate method (the auction method modification) have been developed [10]. The approach based on dynamic programming is used for solving significantly complicated variants of the traveling salesman problem, which are set, in particular, when designing the pattern cutting technologies [11, 12].

An even more common approach to ensuring the precise routing of vehicles is to formulate these tasks as the problems of linear integer and partial integer linear programming [13, 14]. For example, the analysis of selected works on UAV flights optimization, published in the second decade of this century, shows that the share of linear programming methods in searching for accurate solutions is estimated at more than 40 per cent [15]. The approximated methods include an equally significant share of algorithms that are based on genetic metaheuristics, and the next most frequently used type of algorithms is ACO [15]. The evo-



Fig. 3. The Krimean Bridge in Kerch, Russia.



Fig. 4. Adler city, Russia.



Fig. 5. New York city, USA.

lutionary algorithms, in particular the genetic ones, are used for routing other types of autonomous vehicles, taking into account the existing limitations [16], and for pattern cutting [17]. Then linear programming methods and genetic algorithms also play an important role in solving the tasks of optimization of the Earth surface surveys performed by automated remote sensing satellites [18, 19]. In addition, different heuristic methods and their combinations [15] are proposed for controlling the groups of unmanned aerial vehicles, such as a multi-phase iterative algorithm which combines the Monte Carlo method, the greedy algorithm, and other heuristics [20].

The operations related to sequential tracking of several targets, using a research device fixed rigidly on an SPP, can be divided into two main types: tracking a single object and re-pointing, i.e. changing the targets tracked.

The single object tracking algorithms in the Uragan experiment depend on the research objectives and are restricted primarily by the conditions of the object visibility from the ISS, the maximum angles and the maximum speed of the device's sensitive axis rotation. The examples of such algorithms are taking a single photo image of an object, spectrographic survey of a specified object within the entire time interval of its visibility, sequential photography of parts of a relatively large object, etc.

It is assumed that the operations performed by any of possible algorithms to track individual targets have expected start and end time points of tracking, directions of the device's sensitive axis at the beginning and end of tracking, the sum of angles of the sensitive axis rotation within the tracking time, and *information value*, i.e., quantitative assessment of relevance of the scientific data obtained from the target survey [5]. Based on these data, the algorithm for planning the observation of several targets should select the targets and the sequence of transitions between them, taking into account the specified limitations, and when solving some optimization problem, for example, it should maximize the total information value of targets observation or minimize the sum of angles of the device's sensitive axis on condition that the total information value of observations will not fall below a given value.

Targets can be observed simultaneously by several research devices installed on different SPP. Then, each platform should have its own program of observation of some subset of targets from a common list. In this case, tasks are set to optimize some total value, such as the total information value of observations using all the platforms, or the sum of platforms' rotations.

An approach using the linear programming methods, first proposed in [21, 22], is suitable for optimal control of a single platform with scientific equipment installed on it. Observations performed from several controlled platforms within the Uragan space experi-

ment on board the ISS RS were optimized using additional variants of formulations in terms of integer linear programming, based on the analogy with so-called "extended" formulation of the routing problem for several vehicles [5, 23, 24]. In this approach, possible programs of targets observation are made up for each platform, and then the observation programs (one per each platform) are selected from these sets to compile a common optimal solution.

In addition to manned space missions, considerable experience of planning and implementation of surveys of specific terrestrial targets has been accumulated in the control of constellations of automated Earth remote-sensing satellites [18]. The ground services tend to stop participating in the preparation of detailed mission scenarios. Instead, basic planning of surveys and their results delivery to the Earth are carried out jointly by onboard software of satellites within the constellation [19, 25].

A similar approach based on the use of both ground and onboard software for detailed planning of experiments (especially those related to the Earth remote sensing) is applied to the scientific studies organization on board the ISS RS within the Uragan experiment.

Let us consider a relatively simple task of survey of particular ground targets using cameras with long-focus lenses as an example of application of the software designed for the Uragan space experiment. In Fig. 6, the horizontal axis with level 0 conventionally represents the ISS flight trajectory. The flight time is counted (in seconds) along this axis from left to right, starting from the conventional reference point 0. The vertical axis perpendicular to the trajectory reflects the angles (counted in degrees) at which the cameras' axes of sight deviate from the nadir; positive values of angles correspond to the deviation to the left from the path, while the negative values mean deviation to the right.

The recommended 25 targets for photographing are represented as circles in Fig. 6. The horizontal coordinate of each circle is the time point at which the distance between this object and the ISS is minimal; and the vertical coordinate is the angle at which the sight axis of the camera should decline from the nadir at this time point in order to successfully take the photo of the object.

Pointing at the targets and their shooting are carried out within approximately 100 seconds, using three SPP at the same time. One platform is of SOVA-1 type with the maximum rotation rate of 1.5 deg/s and the maximum possible deviation of the camera sight axis from the nadir being 30 deg. The other two platforms are of SOVA-2 type; they provide the maximum rotation rate of 6 deg/s and the maximum deviation of 20 deg from the nadir.

It is required that the camera sight axis on each platform declines at a given angle no later than one

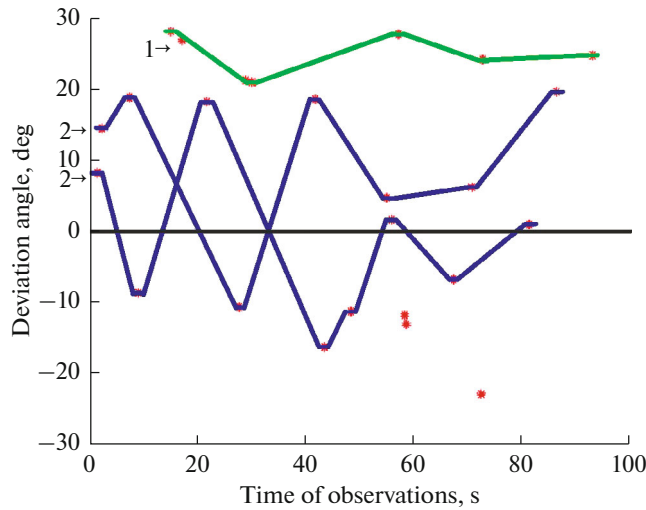


Fig. 6. Graph of shooting of 20 targets out of 25 specified ones (one platform of SOVA-1 type and two platforms of SOVA-2 type are used).

second before the moment of the closest approach of the ISS to the object, and in one second after this moment one may start turning the platform to take a photo of the next object. Thus, photographing takes two seconds.

Considering the above restrictions on the rotation rate of the platforms and on the time of photographing, 8659 possible observation programs were prepared for the SOVA-1 platforms and 241919 ones for the SOVA-2 platforms.

The problem of linear programming was formulated as follows. It was necessary to find binary vector \mathbf{X} that affords a maximum to function

$$I(\mathbf{X}) = \sum_{r=1}^M n_r x_r, \tag{1}$$

where n_r is the number of targets observed according to a program number r .

Vector \mathbf{X} with a length $M = 250578$ elements represents all possible observation programs and is composed by combining vectors \mathbf{X}_1 (with a length of 8659) and \mathbf{X}_2 (with a length of 241919), corresponding to the platform types SOVA-1 and SOVA-2. If the observation program with a particular number r (from 1 to M) has been chosen for observation from a corresponding platform, then the element with this number will take the value of 1 in the vector \mathbf{X} . On the other hand, if this observation program has not been chosen, the element of \mathbf{X} with this number is equal to zero.

Thus, the simplest function of observation information value, equal to the number of observed targets, was used in (1) as a target function.

The number of platforms of each type used was specified by the following conditions:

$$1^T \mathbf{X}_1 \leq 1, \quad 1^T \mathbf{X}_2 \leq 2. \tag{2}$$

It was prohibited to shoot the same object using more than one platform of any type, so the following restriction was applied:

$$\sum_{r=1}^M a_{ir} x_r \leq 1, \quad i = 1, \dots, 25. \tag{3}$$

At the same time, the binary coefficient a_{ir} was formed so that for the first 8659 values of index r the value of a_{ir} is equal to 1 if an object with the number i was chosen for observation from the SOVA-1 platform in the program r ; for the next 241919 values of r the value of a_{ir} is equal to 1 if an object with the number i was chosen for observation from the SOVA-2 platform in the program r . In all other cases, the value of a_{ir} is equal to zero.

As a result of solving this problem by the methods of linear programming, it was found that the maximum possible number of targets that could be photographed under the given conditions was 20, and one of the sets of observation programs which support the survey of this number of targets was also found. This solution is shown in Fig. 6.

Then the task was set to find such a set of observation programs where 20 targets are shot with the minimum sum of rotation angles of all the platforms. In this case, the following function was minimized:

$$R(\mathbf{X}) = \sum_{r=1}^M \theta_r x_r. \tag{4}$$

Here, θ_r is the sum of rotation angles of an SPP for which the program with number r has been prepared.

Along with the limitations (2), (3), the following was taken into consideration:

$$\sum_{r=1}^M n_r x_r = 20. \tag{5}$$

The solution is shown in Fig. 7. The minimum sum of rotation angles is approximately twice less than the sum of rotation angles shown in Fig. 6.

Thus, a two-criterion problem of optimization (which is in many cases also typical of the problems of unmanned aerial vehicles control [15]) has been set and solved. Generally, each of these criteria can be, in turn, composed of a few criteria; for example, the number of observed targets can be replaced with a composite target function of informativity similar to those formulated hereinafter for the RIVR and Hyper-spectrometer scientific equipment.

In the above examples, it turned out to be impossible to take photographs of all specified targets, and the set of photographed targets may change depending on the chosen observation programs. In this case, in order to shoot all the targets within a given time interval, additional platforms are required.

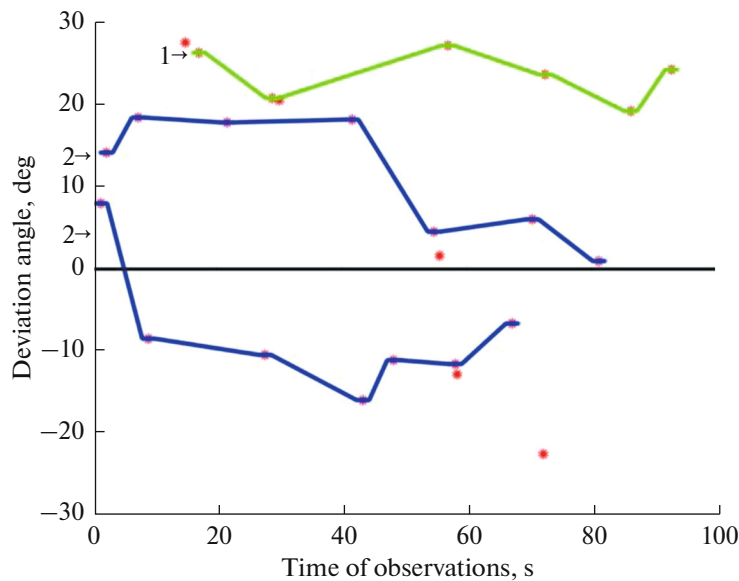


Fig. 7. Graph of shooting of 20 targets out of 25 specified ones with the minimum sum of platforms' rotation angles.

If the number of specified targets and the number of platforms involved in their observation are increased, it may become impossible to obtain an accurate solution of the optimization task within acceptable time. In such cases genetic algorithms are applied [26], which work in accordance with the following general procedure [23].

A definition of genotype \mathbf{Y} is introduced as a combination (concatenation) of three numerical strings, each representing an observation program for one of the three SPP. Since the above example introduces a strict chronological sequence of targets shooting, each observation program can be represented by a binary vector with its components corresponding to the targets from the common list ordered by the time of their observations. The targets selected for shooting are marked with 1, and those not selected—with 0.

The initial generation of population (set of genotypes) is formed randomly, and then the process of evolution is run, where the next generation is formed on the basis of the previous one, using standard operators of crossing, mutation and selection. As a rule, the algorithm is stopped after a specified number of generations has been achieved. During selection, the genotypes with the largest values of the following fitness function are distinguished:

$$F(\mathbf{Y}) = \sum_{i=1}^3 I_i - P_1 N_1 - P_2 N_2, \quad (6)$$

where I_i is the estimate of efficiency of the observation program number i included in the genotype (in this example it is the number of targets observed using an SPP according to the program). Two penalty functions were used, which ensured the quantitative count of violations of specified restrictions.

Firstly, the pairs of targets that could not be observed simultaneously due to the preset restrictions were identified in each sequence of observations within a genotype. The total number N_1 of such violations found in a genotype was counted and multiplied by the amount of penalty P_1 .

Secondly, in the sequences of observations performed by different platforms, the same targets selected for observations were identified. These coincidences were deemed prohibited and their number N_2 was also multiplied by some penalty P_2 .

At the end of the algorithm, the genotype with the maximum value of expression (6) was chosen on condition that the number of violations of both types was equal to zero.

The sums of platform rotation angles were minimized in a similar manner. In this case, in addition to the above penalties, the penalty for deviation of the number of targets from a given value was introduced.

In contrast to the linear programming algorithms, the genetic algorithms cannot guarantee that their result will be optimal in the strict sense. For instance, when special onboard software based on a genetic algorithm with the fitness function (6) was used for solving the problems presented in Fig. 6, the resulting value was the same as that obtained by the linear programming methods. However, when solving the problem shown in Fig. 7, the resulting sum of the platforms' rotation angles was by 4.3% higher than the theoretical minimal value.

Nevertheless, despite the loss of accuracy compared to the linear programming methods, the genetic algorithms can provide quite efficient and practicable solutions within a short time, which is especially

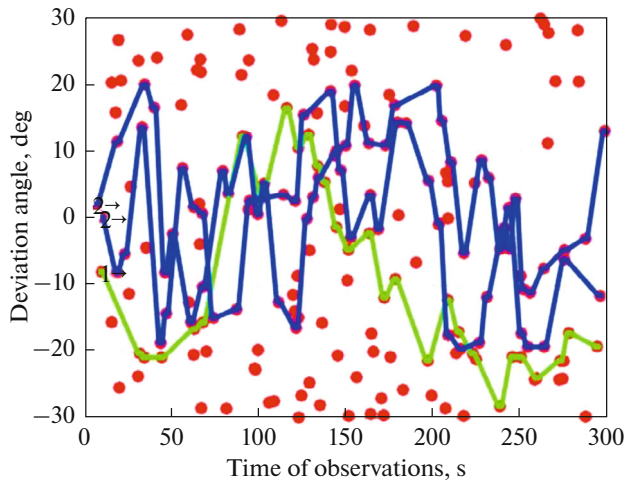


Fig. 8. Graph of shooting 103 of 200 specified targets (one SOVA-1 and two SOVA-2 platforms are used).

important for planning the observation of targets from large catalogues. For example, for a list of 200 targets and an interval of observations lasting 300 s, the task was set to find the largest number of targets that can be observed using one SOVA-1 and two SOVA-2 platforms. A genetic algorithm obtained an estimate of this number, equal to 103, and one of possible sets of programs which make it possible to observe this number of targets. Then another genetic algorithm formed programs with a 2.5 times smaller sum of rotation angles of platforms pointed at 103 targets from 200 specified ones. This solution, suitable for practical application, is shown in Fig. 8.

The software for planning the observation of external targets from onboard the ISS can also solve the problems similar to the multiple traveling salesmen problem, which could occur, for example, in the case of optimization of several astronomical targets observation using a few moving platforms [5]. Similar problems can be set when observing the Earth's surface. Their approximate solutions are found by means of special genetic algorithms without penalty functions, as well as the algorithms based on ACO metaheuristics.

OPTIMIZATION OF OBSERVATION PROGRAM FOR RIVR SCIENTIFIC EQUIPMENT

High-resolution infrared radiometer RIVR is being developed for the Earth monitoring in the middle and far infrared ranges. This equipment is manufactured at the Russian Space Systems enterprise and, taking into account the ISS orbit height, it will provide the world-level information. The equipment has the following basic characteristics [2, 4]:

- number of information channels: 2;

- limits of the spectral ranges of channels by the level 0.5:
 - 3.5–4.1 μm ,
 - 8.0–10.0 μm ;
- spatial resolution from the ISS nominal orbit height (400 km): 30 m;
- field of view for an orbit 400 km high: 70 km;
- difference of temperatures measured at the level of 300, equivalent to noise:
 - in the range of 3.5–4.1 μm : ≤ 0.5 K,
 - in the range of 8.0–10.0 μm : ≤ 0.2 K;
- output information bit depth: at least 10 bit;
- operation mode: sessional.

Functionally, the RIVR equipment consists of two units:

- optoelectronic unit (OEU) generating the video information in two spectral ranges: 3.5–4.1 and 8.0–10.0 μm ;
- radiometer control unit for operating the OEU and interfacing it with the ISS onboard systems.

The OEU is installed on the outer surface of the MLM of the ISS RS, and the radiometer control unit—inside the MLM. The RIVR radiometer uses the principle of multi-row mechanical scanning. Even with a relatively small number of sensitive elements in the radiation detector, this method implements the spatial resolution of 30 m and the field of view of 70 km (angle of sight 10 deg) with the noise-equivalent difference of measured temperatures being at least 0.2 K at the background temperature level of 300 K.

The OEU of the radiometer comprises a flat scanning mirror oscillating with a period of 1.144 s using a low-speed precision drive; a catadioptric lens; spectrum-splitting system and multi-element detectors of radiation. The radiation detectors are Russian multi-element (matrix) IR photodetectors with 4×288 elements, cooled by a microcryogenic system down to cryogenic temperatures (80 K). Their operation time between failures is at least 6000 h. The scanning mirror oscillation axis and the rows of radiation detectors are oriented along the spacecraft flight direction, due to which a microframe with a format of 288×2350 elements can be formed in a single cycle of line scanning by the radiometer. The microframes overlap is 10 to 40 elements. During the on-ground processing, the microframes are geometrically corrected and put together to form a single track image.

The RIVR will be integrated with the information and control system (ICS) of the ISS RS. The ICS will support the transmission of control digital arrays and the distribution of ballistic data. In addition, the ICS will provide for intermediate storage of the information received from the RIVR and its further transmission to the Earth via a broadband communication line.

Using the RIVR radiometer in the Uragan space experiment, it will be possible to obtain trace images in

the IR spectrum, which can be used in a wide range of applications:

- monitoring and prediction of human-made and natural emergencies;
- detection of forest and underground fire foci, large thermal emissions of pollutants into the environment;
- monitoring of natural hydrometeorological phenomena;
- assessment of the soil moisture content and the groundwater levels;
- search for groundwater and geothermal sources;
- research of dynamic processes in water areas;
- various types of thematic mapping of the Earth's surface, including geological mapping (search for mineral resources, their identification, detection of possible oil and gas fields);
- research of volcanic and seismic activity;
- assessment of industrial and domestic waste landfills and their effect on the environment;
- detection of heat emission and pollution sources, etc.

This information will be useful for the Federal Agency of Forest Protection, the Ministry of Emergency Situations, environmental agencies, geological exploration services, as well as regional industries and businesses.

Also, during the space experiment at the ISS RS, it will be possible to test the high-resolution IR radiometer prototype in standard operation conditions for its further use in different automated information systems of remote sensing.

While implementing the research program with the RIVR equipment, several coherent sequences of observation of targets selected from a specified general catalogue can be made up for a specified planning interval up to a few days or weeks. These sequences are traditionally called the observation zones [5].

When planning and conducting the observations using the RIVR scientific equipment, the information value of such zones is calculated as follows:

$$I_j = \sum_{i=1}^N p_i o_i l_i s_i z_{ij}, \quad j = 1, \dots, M,$$

where: M and j are the amount of zones and their numbers; N and i are the amount of all targets in the catalogue and their numbers; p_i is the priority of the i -th object, ($1 \leq p_i \leq 10$); o_i is the cloud cover coefficient when observing the i -th object ($0 \leq o_i \leq 1$); l_i is the illumination coefficient when observing the i -th object; s_i is the coefficient of the object's scanned surface area, $s_i = S_i'/S_i$, where S_i and S_i' are the area of the object and the area of the surveyed part of the object; z_{ij} is a binary indicator of the presence of targets in the experiment zones.

If the i -th object of the catalogue is selected to be observed in the j -th zone, the value of z_{ij} is equal to 1, if not selected—0.

If the i -th object is located on a part of the Earth not illuminated by the Sun, $l_i = 1$. For the targets illuminated by the Sun, $l_i = 0$ if $h_i > h^{\max}$, and $l_i = (h^{\max} - h_i)/h^{\max}$ in all other cases. The value h_i is the angle of the Sun (angular elevation of the Sun above the local horizon) for the i -th object; h^{\max} is the maximum permissible angle of the Sun during the survey.

In the RIVR scientific equipment, the measurements are initially recorded on its own recorder which has a limited volume. The number of the device runs is also limited due to the device's cooling system capacity. We denote the following:

K_j is the number of scientific equipment runs in the j -th zone;

V_j is the amount of information received in the j -th zone;

K^O is the upper limit of the scientific equipment runs;

V^O is the upper limit of the information amount, which depends on the device's recorder capacity;

I^O is the lower limit of the total information value of selected zones;

x_j is the j -th component of the binary vector \mathbf{X} , which is equal to 1 if the j -th zone is selected for the experiment; otherwise it is equal to 0.

During the ISS RS mission, the following tasks can be stated for the survey optimization:

(1) Maximization of information value under given limitations on the number of scientific equipment runs and the amount of information for recording in the scientific equipment recorder. In this case, vector \mathbf{X} that maximizes the target function is to be found:

$$L(\mathbf{X}) = \sum_{j=1}^M I_j x_j$$

under the limitations $\sum_{j=1}^M K_j x_j \leq K^O$ and

$$\sum_{j=1}^M V_j x_j \leq V^O.$$

(2) Minimization of the amount of information to be recorded under the limitations on the information value and on the number of runs. Vector \mathbf{X} minimizing the target function is to be found:

$$L(\mathbf{X}) = \sum_{j=1}^M V_j x_j$$

under the limitations $\sum_{j=1}^M I_j x_j \geq I^O$ and

$$\sum_{j=1}^M K_j x_j \leq K^O.$$

(3) Minimization of the number of runs under the limitations on the information value and on the

Table 1. Information value and resources spent in the zones

Zone	Zone information value	Number of runs	RE recorder filling percentage	Amount of information in the zone, Gb
1	20.10	9	15%	37.50
2	23.70	8	13%	33.33
3	23.45	12	20%	50.00
4	24.95	9	15%	37.50
5	31.85	10	17%	41.67
6	30.85	11	18%	45.83
7	24.50	13	22%	54.17
8	24.50	9	15%	37.50
9	21.85	8	13%	33.33
10	25.50	12	20%	50.00
11	24.33	13	22%	54.17
12	29.05	11	18%	45.83
13	23.70	7	12%	29.17
14	26.20	12	20%	50.00
15	20.45	13	22%	54.17
16	22.75	10	17%	41.67
17	29.10	9	15%	37.50
18	25.55	15	25%	62.50
19	23.35	11	18%	45.83
20	25.60	9	15%	37.50
21	21.95	7	12%	29.17
22	21.10	14	23%	58.33
23	31.30	9	15%	37.50
24	32.40	10	17%	41.67
25	29.35	9	15%	37.50
26	26.80	13	22%	54.17
27	22.55	9	15%	37.50
28	23.95	9	15%	37.50
29	24.90	11	18%	45.83
30	26.25	13	22%	54.17
31	29.00	9	15%	37.50

amount of information to be recorded. Vector \mathbf{X} minimizing the target function is to be found:

$$L(\mathbf{X}) = \sum_{j=1}^M K_j x_j$$

under the limitations $\sum_{j=1}^M I_j x_j \geq I^0$ and $\sum_{j=1}^M V_j x_j \leq V^0$.

As an example, the program of observations for the RIVR equipment, optimized according to the above approach, is described below. The conditions of observations in conducted in July, 2022, were simulated for

real targets of the Uragan and Stsenariy space experiments, including fires.

Information value and spent resources of the zones were calculated for selected targets (see Table 1). One zone was assumed to be 24 h, i.e., every 24 h in July, 2022, were considered. The recorder filling percentage indicated for each zone is the share of the recorder memory occupied by the information that has been received in a given zone.

The problem of information value maximization was solved under the limitations on the number of scientific equipment runs and the amount of information to be recorded on the scientific equipment's recorder. To accelerate the verification, simple limitations on

the number of scientific equipment runs ($K^O = 300$) and the amount of information to be recorded in the own memory of the scientific equipment ($V^O = 1300$):

$$\mathbf{X} = \{1, 1, 1, 1, 1, 1, 1, 1, 1, 1, 1, 1, 1, 0, 1, 1, 1, 1, 1, 0, 1, 1, 1, 1, 1, 1, 1, 1\},$$

$$L(\mathbf{X}) = 749.325.$$

For verification, the solution was also obtained by means of computer search for all options. When the optimal solution is found this way, it takes by three orders of magnitude more running time. When the number of zones or the number of targets in the zones is further increased, and if more limitations are added, the speed difference between both methods of solution will increase as well, and as a result, it will be impossible to solve this problem by direct search on a common personal computer.

OPTIMIZATION OF THE PROGRAM OF OBSERVATIONS USING THE HYPERSPECTROMETER RE

Currently, within the framework of the Uragan space experiment, the Hyperspectrometer scientific equipment has been created and is being prepared for transportation to the ISS RS to further develop the Earth monitoring system [2]. The Hyperspectrometer scientific equipment is designed for astronauts to survey the Earth surface. This equipment was made by the Moscow Institute of Physics and Technology (MIPT) and Lepton Scientific and Production Association. Astronauts can process the survey data on board, using the Hyperspectrometer. This will accelerate the analysis of the received data, improve the quality of observation planning, and reduce the data flows that are promptly transmitted to the Earth.

The equipment is designed for recording and processing the hyperspectral images of the Earth surface in several spectral channels (at the astronaut's choice from 1 to 100 out of 180 channels) in the visible range and near infrared range of the spectrum, as well as for obtaining panchromatic images to visualize a given area of the Earth surface.

Using the Hyperspectrometer RE, it is planned to solve the following tasks:

- state assessment of forests;
- state assessment of agricultural plantations;
- search and evaluation of the concentration of various minerals in exposed soil areas;
- detection of vegetation and water pollution with oil, fuel oil, etc., as well as assessment of respective damage;
- mapping of chlorophyll concentration in near-surface waters;
- detection of sites of narcotic plants among other vegetation, etc.

An approach similar to the one developed for the surveys with the RIVR scientific equipment was used to plan the observations with the Hyperspectrometer. At the same time, it should be noted that the Hyperspectrometer is installed on the porthole no. 9 of the service module, and the personnel are required for its installation, disassembly, or operation in the manual mode when control commands need to be issued (setting the angles of pointing, start time and end time of survey). Therefore, the working time of the crew during the experiments with the Hyperspectrometer, and the time interval for using the porthole no. 9 which is required for other studies as well, are considered as essential resources. Since the device operates in the visible and near infrared ranges, it can only be used when the survey targets are illuminated.

The information value of the j -th zone when using the Hyperspectrometer has the form:

$$I_j = \sum_{i=1}^N p_i o_i l_i s_i z_{ij}, \quad j = 1, \dots, M.$$

In this case, $l_i = 1 - |h_i^{opt} - h_i| / h_i^{opt}$, where h_i and h_i^{opt} are the angle of the Sun and the optimal angle of the Sun for the i -th object. All other parameters are similar to those used in calculating the information value of the observation zones for the RIVR.

To optimize the observation program using the Hyperspectrometer, it is necessary to find binary vector \mathbf{X} that maximizes the target function

$$L(\mathbf{X}) = \sum_{j=1}^M I_j x_j$$

under the limitations $\sum_{j=1}^M T_j x_j \leq T^O$, $\sum_{j=1}^M \tau_j x_j \leq \tau^O$ and $\sum_{j=1}^M V_j x_j \leq V^O$, where: T_j is the time of the crew's work with the scientific equipment in the j -th zone; T^O is the limitation on the time of the crew involvement in the scientific equipment operation within the interval of planning; τ_j is the time interval during which the porthole no. 9 is used in the j -th zone; τ^O is the limitation on the time of using the porthole no. 9 for survey with the Hyperspectrometer within the interval of planning.

When preparing the observation program for the Hyperspectrometer, the conditions for the observations were simulated for June 2022. Similarly to the previous example, the targets were taken from the list of targets of the Uragan, Stsenariy and Dubrava space experiments.

The information value and expendable resources of the zones were calculated. One working day was assumed to be a zone for manual control of the equipment with the involvement of the crew.

For the automatic operation mode of the Hyperspectrometer, an example of solution is given where the program information value is maximized in the

- scientific equipment of the International Space Station to objects under study, *Cosmic Research*, 2022, vol. 60, no. 1, pp. 58–66.
<https://doi.org/10.1134/S0010952522010014>
6. Stefanov, W.L., Evans, C.A., Runco, S.K., Wilkinson, M.J., Higgins, M.D., and Willis, K., Astronaut photography: Handheld camera imagery from low Earth orbit, in: *Handbook of Satellite Applications*, Pelton, J., Madry, S., Camacho-Lara, S. (eds.), New York, NY: Springer, 2016, pp. 683–728.
https://doi.org/10.1007/978-1-4419-7671-0_39
 7. Belyaev, B.I., Belyaev, M.Yu., Sarmin, E.E., Gusev, V.F., Desinov, L.V., Ivanov, V.A., Krot, Yu.A., Martinov, A.O., Ryazantsev, V.V., and Sosenko, V.A., Design and flight tests of science hardware video-spectral system on board the Russian segment of the ISS, *Kosmicheskaya tekhnika i tekhnologii*, 2016, vol. 13, no. 2, pp. 12–20.
 8. Belyaev, M.Yu., Belyaev, B.I., Ivanov, D.A., Katkovskii, L.V., Martinov, A.O., Ryazantsev, V.V., Sarmin, E.E., Silyuk, O.O., and Shukailo, V.G., Atmospheric correction of data registered on board the ISS. Part I. Methodology for spectra, *Sovremennye problemy distantsionnogo zondirovaniya Zemli iz kosmosa*, 2018, vol. 15, no. 6, pp. 213–222.
<https://doi.org/10.21046/2070-7401-2018-15-6-213-222>
 9. Belyaev, M.Yu., Belyaev, B.I., Ivanov, D.A., Katkovskii, L.V., Martinov, A.O., Ryazantsev, V.V., Sarmin, E.E., Silyuk, O.O., and Shukailo, V.G., Atmospheric correction of data registered on board the ISS. Part II. Methodology for images and application results, *Sovremennye problemy distantsionnogo zondirovaniya Zemli iz kosmosa*, 2018, vol. 15, no. 6, pp. 223–234.
<https://doi.org/10.21046/2070-7401-2018-15-6-223-234>
 10. Aleksanin, A.I., Shcherbatyuk, A.F., On monitoring of marine fishing areas using satellite data and information from marine robotic systems, *Upravlenie bol'shimi sistemami*, 2022, vol. 100, pp. 237–260.
<https://doi.org/10.25728/ubs.2022.100.11>
 11. Petunin, A.A., Chentsov, A.G., and Chentsov, P.A., *Optimal'naya marshrutizatsiya instrumenta mashin figurnoi listovoi rezki s chislovyim programmym upravleniem. Matematicheskie modeli i algoritmy* (Optimal Routing of the Tool of Profile-Cutting Machine with Numerical Program Control. Mathematical Models and Algorithms), Ekaterinburg: Izdatel'stvo Ural'skogo Universiteta, 2020.
 12. Chentsov, A.G., Chentsov, A.A., and Seseikin, A.N., *Zadachi marshrutizatsii peremeshchenii s neadditivnym agregirovaniem zatrat* (Routing Problems with Non-Additive Cost Aggregation), 2nd Edition (Reprint), Moscow: LENAND, 2021.
 13. Cheikhrouhou, O., Khoufi, I., A comprehensive survey on the Multiple Travelling Salesman Problem: Applications, approaches and taxonomy, *Computer Science Review*, 2021, vol. 40, 100369.
<https://doi.org/10.1016/j.cosrev.2021.100369>
 14. Jayarathna, D.G.N.D., Lanel, G.H.J., and Juman, Z.A.M.S., Survey on ten years of multi-depot vehicle routing problems: Mathematical models, solution methods and real-life applications, *Sustainable Development Research*, 2021, vol. 3, no. 1, pp. 36–47.
<https://doi.org/10.30560/sdr.v3n1p36>
 15. Vilorio, D.R., Solano-Charris, E.L., Munoz-Villamizar, A., and Montoya-Torres, J.R., Unmanned aerial vehicles/drones in vehicle routing problems: A literature review, *International Transactions in Operational Research*, 2020, vol. 28, pp. 1626–1657.
<https://doi.org/10.1111/itor.12783>
 16. Kenzin, M.Yu., Bychkov, I.V., and Maksimkin, N.N., Mobile robots group coordination during long-term comprehensive monitoring, *Proc. XIII All-Russian Meeting on Control Problems (VSPU-2019)*, Moscow: IPU RAN, 2019, pp. 2351–2356.
<https://doi.org/10.25728/vspu.2019.2351>
 17. Yu, W., Lu, L., A route planning strategy for the automatic garment cutter based on genetic algorithm, *Proc. 2014 IEEE Congress on Evolutionary Computation (CEC)*, Beijing, China, 2014, pp. 379–386.
<https://doi.org/10.1109/CEC.2014.6900425>
 18. Malyshev, V.V., Darnopykh, V.V., *Operativnoe planirovanie tselevogo funktsionirovaniya kosmicheskikh sistem nablyudeniya i svyazi* (Executive Planning of Target Functioning of Space Observation and Communication Systems), Moscow: Izdatel'stvo MAI, 2017.
 19. Zhang, G., Li, X., Hu, G., Zhang, Z., An, J., and Man, W., Mission planning issues of imaging satellites: Summary, discussion, and prospects, *International Journal of Aerospace Engineering*, 2021, vol. 2021, Article ID 7819105.
<https://doi.org/10.1155/2021/7819105>
 20. Maksimov, A.N., Maksimov, N.A., Development and description of mathematical model of unmanned aerial vehicles group flight, *Proc. International Scientific Conference "Advanced Information Technologies" (PIT 2018)*, S.A. Prokhorov, Ed., Samara: Samara Science Center of the RAS, 2018, pp. 487–490.
 21. Belyaev, M.Yu., The main tasks and principles of designing a ground-onboard complex for controlling experiments carried out using spacecraft, *Upravlyayushchie sistemy i mashiny*, 1980, no. 4, pp. 103–107.
 22. Belyaev, M.Yu., Operational planning of research experiments performed using spacecraft, *Kosmicheskije issledovaniya*, 1980, no. 2, pp. 235–241.
 23. Belyaev, M.Yu., Borovikhin, P.A., Karavaev, D.Yu., and Rasskazov, I.V., Optimization of scientific equipment guidance to objects under study from onboard a large-sized orbital station, *Proc. XIV All-Russian Multi-conference on Control Problems (MKPU-2021)*, Rostov-on-Don, 2021, vol. 3, pp. 70–72.
 24. Toth, P., Vigo, D., *Vehicle Routing. Problems, Methods, and Applications*, 2nd Edition, Philadelphia: Society for Industrial and Applied Mathematics, Mathematical Optimization Society, 2014.
 25. Gorodetskii, V.I., Karsaev, O.V., Distributed surveillance system based on self-organized collective behavior of small satellite cluster, *Izvestiya YuFU. Tekhnicheskije nauki*, 2017, vol. 187, no. 2, pp. 234–247.
<https://doi.org/10.18522/2311-3103-2017-1-234247>
 26. Simon, D., *Evolutionary Optimization Algorithms*, Hoboken, NJ: John Wiley & Sons, 2013.
 27. Belyaev, M.Yu., From the R-7 missile and the first manned mission into space up to permanently manned orbital station, *Gyroscopy and Navigation*, 2021, vol. 12, no. 3, pp. 265–280.
<https://doi.org/10.1134/S2075108721030032>

Publisher's Note. Pleiades Publishing remains neutral with regard to jurisdictional claims in published maps and institutional affiliations.